Controllable synthesis and enhanced gas sensing performances of AuNP-modified $ZnSnO_3$ hollow nanocubes toward highly sensitive toluene detection

Jun Li [a], Yongjiao Sun [a], Zhaomin Tong [b,c], Zhenting Zhao [a], Wendong Zhang [a], Jie Hu [a] and Lin Chen [d*]*

[a] *Center of Nano Energy and Devices, College of Information and Computer, Taiyuan University of Technology, Taiyuan 030024, Shanxi, China*

[b] *State Key Laboratory of Quantum Optics and Quantum Optics Devices, Institute of Laser Spectroscopy, Shanxi University, Taiyuan, Shanxi 030006, China*

[c] *Collaborative Innovation Center of Extreme Optics, Shanxi University, Taiyuan, Shanxi 030006, China*

[d] *Key Laboratory of Interface Science and Engineering in Advanced Materials (Taiyuan University of Technology), Ministry of Education, Taiyuan 030024, China*

**Author for correspondence. E-mail: hujie@tyut.edu.cn (J. Hu); chenlin01@tyut.edu.cn (L. Chen)*

S1: XPS survey spectrum of $Au_2NPs@ZnSnO_3$ nanostructures

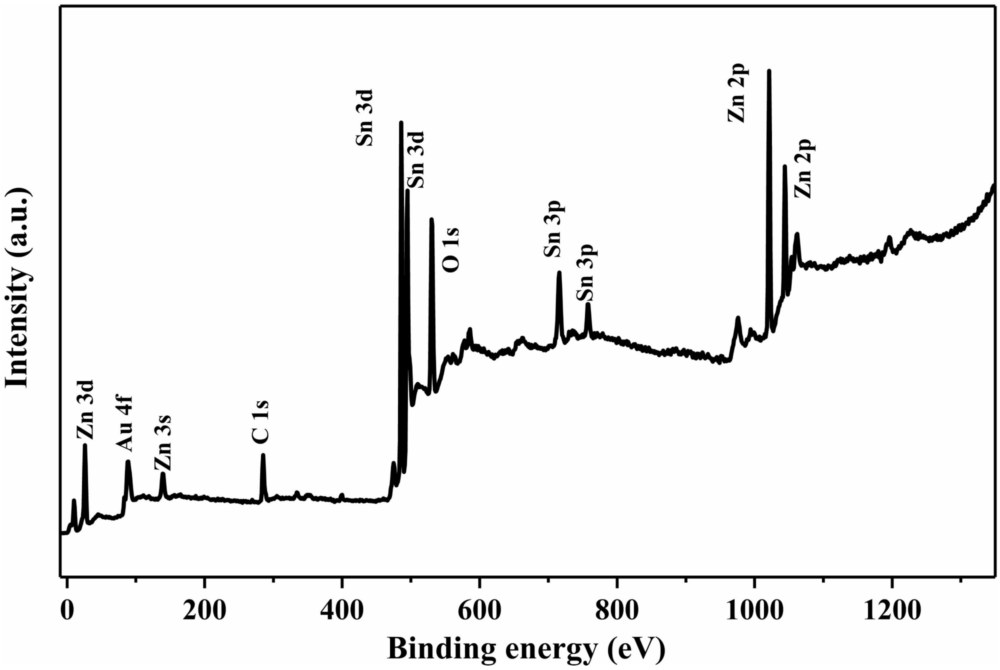

Fig. S1. The full survey spectrum of the $Au_2NPs@ZnSnO_3$ nanostructure

Fig. S1 illustrated the full survey spectrum of $Au_2NPs@ZnSnO_3$ nanostructure ranging from 0~1300 eV, and the measured results exhibited the existence of Zn, Sn, O and Au elements. Meanwhile, there is no other impurity elements appearance in the full survey spectrum, which indicates high-purity of AuNP-modified $ZnSnO_3$ samples.

S2: Gas sensing performances of $ZnSnO_3$ sensors

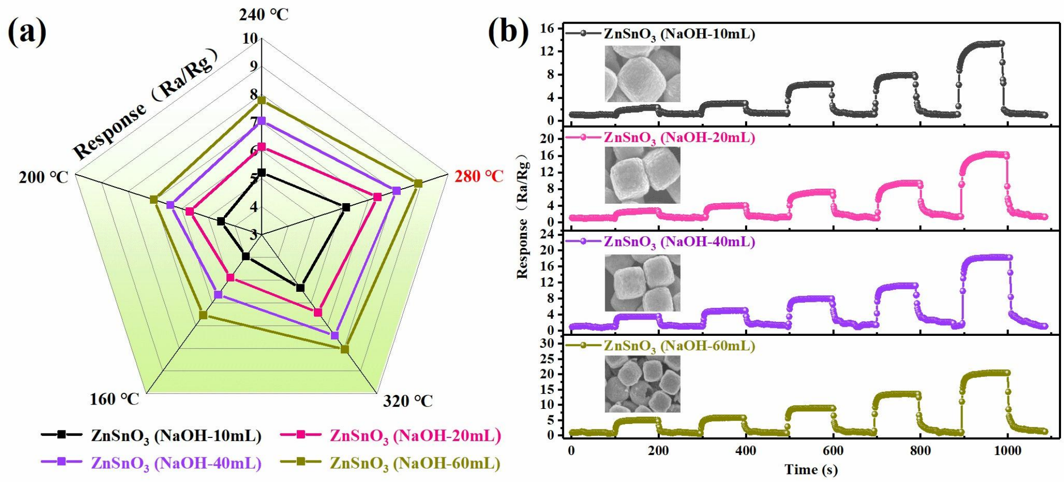

Fig. S2 (a) Gas sensing performances as-prepared $ZnSnO_3$ sensors toward 100 ppm toluene under different operating temperatures. (b) Dynamic response-recovery curves of as-prepared pure $ZnSnO_3$ sensors toward 20-400 ppm toluene at 280°C.

Fig. S2 (a) shows the sensor radar plots of as-prepared $ZnSnO_3$-based gas sensors with different NaOH-assisted dissolution. The optimum operating temperature was investigated on all the as-prepared gas sensors, which selected the 280°C as the working temperature. Furthermore, gas sensor $ZnSnO_3$ with the volume NaOH-assisted dissolution of 60 mL shows the best response among all the as-prepared gas sensors. Fig. S2 (b) illustrates the dynamic cycle of $ZnSnO_3$ sensors toward 20-400 ppm toluene at 280°C, and the excellent gas sensing performances of $ZnSnO_3$ (NaOH-60 mL) sensor can be attributed the larger surface area of unique hollow nanocubes.

S3: Sensor response of Au_xNPs@$ZnSnO_3$ under different concentrations of toluene

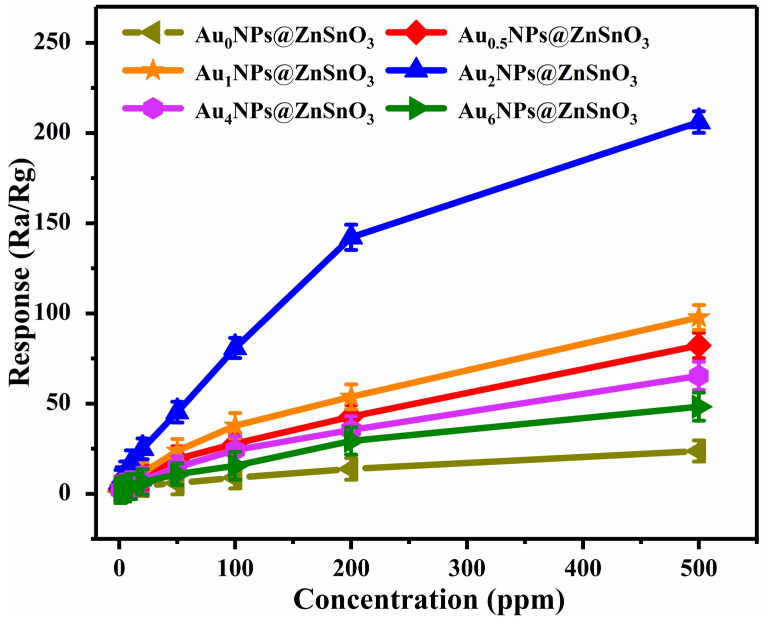

Fig. S3 Response-concentration curves of as-fabricated Au_xNPs@$ZnSnO_3$ gas sensors toward different concentrations of toluene under their optimum working temperature.

Fig. S3 plots the response-concentration curves of as-fabricated Au_xNPs@$ZnSnO_3$ sensors toward different concentrations of toluene. Obviously, all the sensor responses were increasing with the increase concentration of toluene at the optimum working temperature. Moreover, the as-fabricated Au_2NPs@$ZnSnO_3$ sensor showed the highest response than other sensors under the same concentration of toluene.

S4: Sensor response of $Au_xNPs@ZnSnO_3$ toward low concentration of toluene

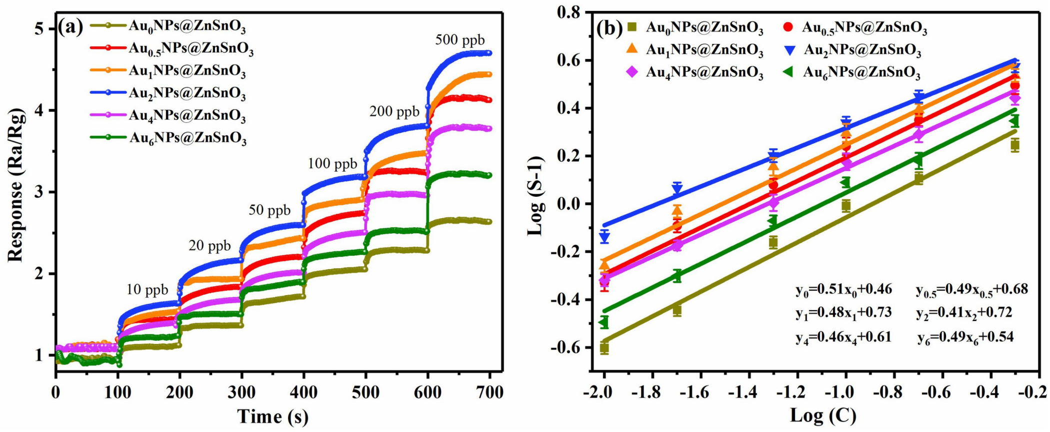

Fig. S4 Dynamic response-recovery curves (a) and linear relationship fitting curves (b) of as-fabricated $Au_xNPs@ZnSnO_3$ sensors to 10-500 ppb toluene at their optimum working temperature.

Fig. S4 (a) displays the as-fabricated $Au_xNPs@ZnSnO_3$ sensors were exposed to a continuous concentration of toluene from 10 to 500 ppb under their optimal operating temperature. The measured results reveal that all the sensor responses of $Au_xNPs@ZnSnO_3$ were enhanced with the increasing concentration from 10 to 500 ppb.

Expectedly, the $Au_2NPs@ZnSnO_3$ sensor exhibited the highest response than other sensors, which was consistent well with the sensor responses under high concentration of toluene. Meanwhile, Fig. S4(b) displays the corresponding linear relationship fitting curves of $Au_xNPs@ZnSnO_3$ sensors, and the measured linear relationship of $Au_2NPs@ZnSnO_3$ sensor is $y_2 = 0.41x_2 + 0.72$, which showed good linear relationship toward ppb-level of toluene detection.

S5: Humidity effects of as-fabricated $Au_xNPs@ZnSnO_3$ sensors

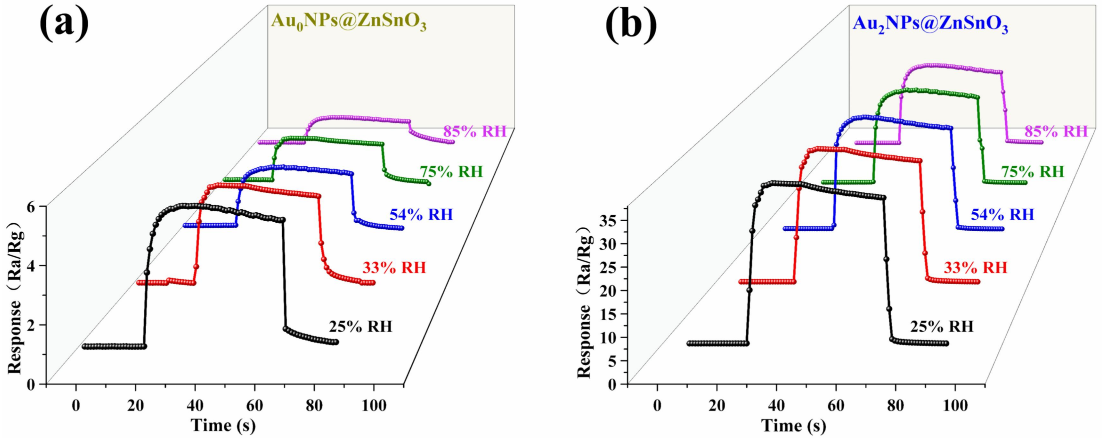

Fig. S5 (a-b) Response curves of $Au_0NPs@ZnSnO_3$ and $Au_2NPs@ZnSnO_3$ sensors toward 50 ppm toluene under different humidity conditions.

Furthermore, the humidity effects were also conducted on the as-fabricated $Au_0NPs@ZnSnO_3$ and $Au_2NPs@ZnSnO_3$ sensors toward 50 ppm toluene under their optimum working temperatures. Obviously, the sensor responses gradually decreased with the increasing of humidity from 25% RH to 85% RH, and the results showed the humidity can significantly influence gas sensing properties. Meanwhile, the $Au_2NPs@ZnSnO_3$ sensor presented good anti-humidity property compared with $Au_0NPs@ZnSnO_3$ sensor. The possible reasons may be ascribed to the good chemical catalytic effect of AuNPs, which can greatly enhance absorption toluene and oxygen molecules.